Applied Energy 148 (2015) 23–31

Contents lists available at ScienceDirect

Applied Energy

journal homepage: www.elsevier.com/locate/apenergy

Systematic approach to determination of optimum gas-phase mass transfer rate for high-gravity carbonation process of steelmaking slags in a rotating packed bed

Shu-Yuan Pan [a], Elisa G. Eleazar [b], E-E Chang [c], Yi-Pin Lin [a], Hyunook Kim [d], Pen-Chi Chiang [a,*]

[a] Graduate Institute of Environmental Engineering, National Taiwan University, 71 Chou-Shan Rd., Taipei City, Taiwan 10673, Taiwan, ROC
[b] Department of Chemical Engineering, Mapua Institute of Technology, Muralla St., Intramuros, Manila 1002, Philippines
[c] Department of Biochemistry, Taipei Medical University, 250 Wu-Hsing Street, Taipei City, Taiwan 110, Taiwan, ROC
[d] Department of Energy and Environmental System Engineering, University of Seoul, 163 Seoulsiripdaero, Dongdaemun-gu, Seoul 130-743, Republic of Korea

HIGHLIGHTS

- Mass transfer models of carbonation in RPB were developed based on two-film theory.
- Correlation between dimensionless groups and $K_G a$/HTU was experimentally determined.
- Effects of different operating variables such as ω, Q_s, Q_G, and L/S were evaluated.
- RSM was introduced for confirming mass transfer model from statistic point of view.
- Optimal operating modulus were graphically determined based on both models and RSM.

GRAPHICAL ABSTRACT

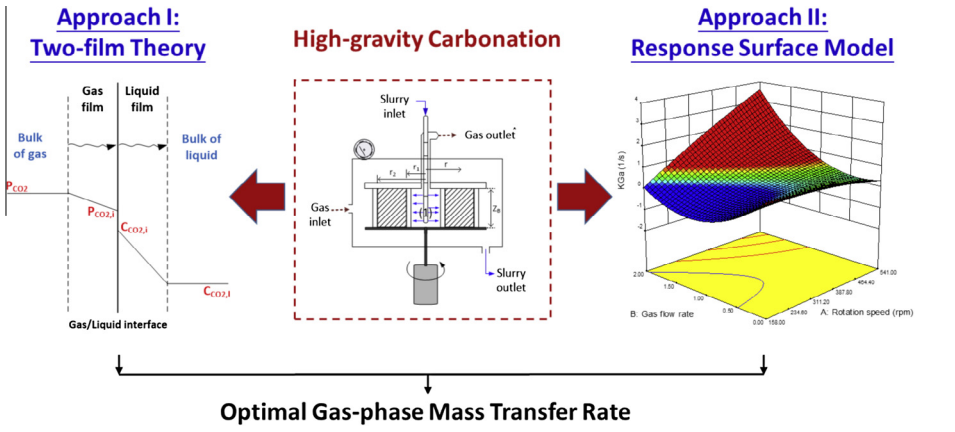

ARTICLE INFO

Article history:
Received 22 December 2014
Received in revised form 14 February 2015
Accepted 6 March 2015
Available online 25 March 2015

Keywords:
CO_2 capture
Process intensification
Mineralization
Two-film theory
Model
Response surface methodology

ABSTRACT

In order to reduce CO_2 emissions and waste generation from the steelmaking industry, a high-gravity carbonation process via rotating packed bed (RPB) was developed using cold-rolling mill wastewater (CRW) and basic oxygen furnace slag (BOFS). Since mass transfer among phases is believed to be a key to effective carbonation for CO_2 fixation, in this study, a mass transfer model for the high-gravity carbonation process was developed based on two-film theory. The mass transfer characteristics including overall gas-phase mass transfer coefficient ($K_G a$) and height of a transfer unit (HTU) were determined accordingly. The results indicated that the mass transfer resistance of carbonation using BOFS/CRW in an RPB was mainly lay on the liquid side. In addition, the effect of key operating variables such as rotating speed, slurry flow rate, gas flow rate, and liquid-to-solid (L/S) ratio on mass transfer characteristics was evaluated. The developed model was validated with the experimental data, where the experimental $K_G a$ values lay within ±20% of the values estimated. Based on the obtained results, empirical models of $K_G a$ and HTU values were established. Furthermore, response surface methodology (RSM) was applied to optimize the high-gravity carbonation process from the viewpoint of mass transfer characteristics. The obtained

* Corresponding author. Tel.: +886 23622510; fax: +886 23661642.
E-mail address: pcchiang@ntu.edu.tw (P.-C. Chiang).

http://dx.doi.org/10.1016/j.apenergy.2015.03.047
0306-2619/© 2015 Elsevier Ltd. All rights reserved.

RSM results were in fairly good agreement with the results of the developed model based on the two-film theory. Based on the theoretical models and statistical analyses, the optimum gas-phase mass transfer rate for high-gravity carbonation process of steelmaking slags in an RPB was graphically determined.
© 2015 Elsevier Ltd. All rights reserved.

1. Introduction

The CO_2 mineralization by accelerated carbonation has been regarded as diffusion controlled reaction (i.e., mass-transfer limited) according to the findings reported in the literature [1–3]. Therefore, different types of approaches such as physical intensification [4] and bio- or chemical activation [5,6] were recently carried out to improve the mass transfer and reaction kinetics. Based on this idea, a rotating packed bed (RPB) reactor has been introduced to improve the mass transfer rate among phases due to its high centrifugal forces and great micro-mixing ability. RPB, the so-called "high-gravity" (sometimes called the "HIGEE") process, is designed to generate high acceleration via centrifugal force, thereby enhancing mass transfer between gas and liquid, and even between liquid and solid. Since RPB can provide a mean acceleration of hundreds, and even thousands, of times greater than the force of gravity, it can effectively lead to the formation of thin liquid films and micro- or nano-droplets [7–9]. Therefore, the volumetric gas–liquid mass transfer coefficients are an order of magnitude higher than those in a conventional packed bed, leading to dramatic reductions in equipment size over that required for equivalent mass-transfer in a gravity flow packed bed [7,9,10].

According to previous studies [11–13], performance of the high-gravity carbonation process using an RPB was found to be better than that using an autoclave or slurry reactor. The CO_2 removal efficiency in the flue gas by alkaline steelmaking wastes in the RPB process was more than 96% with a short retention time (less than 1 min) under ambient temperature and pressure conditions [13]. Precipitation is usually a very fast process and the mixing, especially micro-mixing, of the process is very important for particle size distribution [14]. In such a case, the precipitation process would be controlled by the intrinsic reaction kinetics due to both the excellent micro-mixing [15] and the fine BOFS with a particle size of 44–88 μm in an RPB [11,13,16]. Therefore, before the passive layers around particles are formed, the minerals in BOFS can be rapidly dissolved into solution when the BOFS moved though the packed bed. In other words, the mass transfer between liquid and solid phases may not be the rate limiting factor in the high-gravity carbonation system. In addition, the reaction mechanisms and kinetics of carbonation in an RPB have been studied using shrinking core model [11] and surface coverage model [17], which indicate that the film diffusion should be one of the key rate-limiting steps in the high-gravity carbonation system.

Over the past years, several theoretical models have been developed for describing mass transfer phenomena of RPB for various applications, especially for gas–liquid separation [18,19], which was the earliest designed process. However, sophisticated assumptions and complicated partial differential equation programming were generally required. In addition, no major studies on gas–liquid or liquid–solid mass transfer for the high-gravity carbonation process of alkaline solid wastes have appeared in the literature so far. Therefore, development of an accurate and precise model in which only algebraic equations are included is essential to optimize the high-gravity carbonation process.

The objectives of this study were to (1) develop mass transfer models for high-gravity carbonation of alkaline wastes in an RPB based on theoretical theory, (2) determine the mass transfer characteristics such as the overall gas-phase mass transfer coefficient (K_Ga) and height of a transfer unit (HTU); (3) evaluate the effect of key operating variables such as rotating speed, slurry flow rate and liquid-to-solid (L/S) ratio on mass transfer characteristics; (4) establish a statistical prediction model via response surface methodology (RSM) using experimental data, and (5) optimize the high-gravity carbonation process through a graphical presentation according to the results of the theoretical models and RSM.

2. Materials and methods

2.1. Materials

The ground basic oxygen furnace slag (BOFS) was provided by China Steel Corporation (CSC) (Kaohsiung, Taiwan). The ground BOFS was dried in an oven at 105 °C overnight to eliminate moisture and then stored at room temperature in large airtight containers. The specific gravity of BOFS was 3.14 g/cm^2, with a mean particle size of 12.7 μm. The BOFS was rich in CaO (~43%) and Fe_2O_3 (~29%), with minor component of SiO_2 (~13%) and MgO (~6%). The $Ca(OH)_2$ and free-CaO contents were found to be 7.7% and 1.0%, respectively.

Cold-rolling mill wastewater (CRW) was introduced in the carbonation reaction. The pH value of the CRW was in the range of 8.9–12.2. The major chemical components of CRW were sodium ions (~860 mg/L), potassium ions (~93 mg/L), chloride ions (~2430 mg/L) and sulfate ions (~240 mg/L). Moreover, the concentrations of calcium and magnesium ions were around 4.5 ppm and 0.5 ppm, respectively, of which their contribution to CO_2 mineralization could be neglected. The conductivity of the fresh CRW was approximately 10,000 μmho/cm. It was noted that the CRW can increase the leaching rate and capacity of calcium ions from BOFS into solution, thereby enhancing the carbonation efficiency [12,16,20].

2.2. Specifications of rotating packed bed

In this study, high-gravity *ex-situ* carbonation was performed in a small pilot-scale RPB. The rotation type of packed bed in this study was horizontal rotation, where the gas and slurry were mixed counter-currently within the RPB. The packing zone, where stainless steel wire acted as a packing material, had an inner diameter of 20.5 cm and an outer diameter of 62.5 cm, corresponding to an arithmetic mean radius of 46.5 cm. The axial height of the packed bed was 19.9 cm. In this case, the designed capacity of gas flow in the RPB was around 2.5 m^3/min. In addition, the liquid distributor consisted of a tube with two vertical sets of holes spaced 180° apart. Each hole had a diameter of 0.1 cm, and the holes were spaced at intervals of 0.6 cm. Moreover, the designed liquid loading was 0.009–0.021 m^3/(m^2 min).

2.3. Carbonation experiments

In the experiments, *ex-situ* carbonation was carried out by the high-gravity RPB process using a hot-stove gas at the No. 3 blast furnace plant in CSC (Kaohsiung, Taiwan). The flue gas of the hot

Nomenclature

A	rotation speed (rpm), used in response surface model
a_m	mean acceleration (m s^{-2})
a_e	effective surface area per unit volume of packed bed (gas–liquid interfacial) (m^2 m^{-3})
a_w	wetted surface area of packing (m^2 m^{-3})
a_t	specific surface area of packing (m^2 m^{-3})
B	gas flow rate (m^3/min), used in response surface model
C	slurry flow rate (L/min), used in response surface model
C_G^*	saturation concentration of CO_2 in solution (mg/L)
C_G'	concentration of CO_2 in solution (mg/L)
$C_{G,i}$	CO_2 content in inlet gas streams (%)
$C_{G,o}$	CO_2 content in outlet gas streams (%)
D	L/S ratio (w/w), used in response surface model
D_G	diffusivity of CO_2 in air (m^2 s^{-1})
D_L	diffusivity of CO_2 in water (m^2 s^{-1})
d_p	effective diameter of packing (m)
g	acceleration (m s^{-2})
H	Henry's law constant
h	height of packing bed (m)
I	enhancement factor (–)
$K_G a_e$	overall volumetric mass transfer coefficient (s^{-1})
k_G	gas-side mass transfer coefficient (m s^{-1})
k_L	liquid-side mass transfer coefficient (m s^{-1})
M_G	gas mass flow rate (kg s^{-1})
$Q_{G,i}$	volumetric flow rate of inlet gas (m^3/min), assumed to be equal to Q_G
$Q_{G,o}$	volumetric flow rate of exhaust gas (m^3/min)
Q_{sl}	Slurry flow rate (L/min)
r_i	inside radius of packed bed (m)
r_o	outside radius of packed bed (m)
t'	characteristic time of carbonation (s)
V	volume of packed bed (m^3)

Greek letters

ε	porosity (–), i.e., 0.991
μ_L	viscosity of liquid (kg m^{-1} s^{-1})
$\rho_{CO_2,i}$	CO_2 mass density at the temperature of inflow gas streams (g L^{-1})
$\rho_{CO_2,o}$	CO_2 mass density at the temperature of exhaust gas streams (g L^{-1})
ρ_L	density of liquid (kg m^{-3})
σ_c	surface tension of packing (kg s^{-2})
σ_L	surface tension of water (kg s^{-2})
ω	rotational speed (rad s^{-1})
ω'	rotational speed (rpm)
η	CO_2 removal efficiency (%)
η_{max}	maximum CO_2 removal efficiency (%)

Dimensionless Groups

Re	Reynolds number
Sc	Schmidt number
Gr	Grashof number
We	Weber number
Fr	Froude number

stove containing ~30 vol.% CO_2 flowed inward from the outer edge of the RPB under a slightly positive pressure driving force, while the BOFS/CRW slurry was pumped from the repository to the inner edge of the RPB. The slurry moved outward and left from the outer edge of the RPB under centrifugal force. The slurry was discharged from the bottom of the RPB, whereas the CO_2 exhaust streams were expelled from the top. In addition, the flow type of the BOFS slurry in the RPB was a once-through operation. The schematic diagram of the RPB process was similar to a previous study reported in the literature [12,17].

The important operating parameters include gas flow rate (m^3/min), slurry flow rate (L/min), L/S ratio (L/kg), and rotation speed (rpm). According to previous experience, the optimal value of L/S ratio for BOFS/CRW slurry was observed to range between 10 L/kg and 20 L/kg. In the meantime, the gas flow rate was set to range from 0.33 m^3/min to 0.88 m^3/min. Therefore, the gas-to-liquid (G/L) ratios can be varied from 40 to 140. In addition, CO_2 concentrations in the inlet and exhausted gas streams were measured using an NDIR CO_2 analyzer (Fuji, ZRJ CO_2 Analyzer), with the measurement range from 0% to 100% and a resolution of 0.1%.

2.4. Model development

According to the previous study [13], the CO_2 consumption in bulk solution was mainly attributed (over 98% contribution) to carbonation reaction with calcium ions in solution leached from the steel slag to form calcium carbonate precipitates, where the stoichiometric formula was briefly presented as Eq. (1):

$$Ca^{2+}_{(aq)} + CO^{2-}_{3(aq)} \rightarrow CaCO_{3(s)} \quad (1)$$

In this study, the CO_2 removal efficiency (η) for the high-gravity carbonation process was calculated as Eq. (2):

$$\eta(\%) = \frac{(\rho_{CO_2,i} Q_{G,i} C_{G,i} - \rho_{CO_2,o} Q_{G,o} C_{G,o})}{\rho_{CO_2,i} Q_{G,i} C_{G,i}} \times \% \quad (2)$$

For determining the gas-phase mass-transfer coefficient in a heterogeneous system containing the gas, liquid, and solid phases, the following assumptions were made:

(1) The effect of an inclined gas–liquid interface is neglected.
(2) The concentration of the liquid at the particle surface is equal to the saturation concentration of the solution. In other words, the mass transfer between the liquid and the solid is neglected.
(3) The changes in size and surface area of solid particles are neglected.
(4) Solid distribution throughout the bed is uniform.
(5) The Grashof (Gr) number is determined by the mean radius of the packed bed.

In general, the $K_G a$ in a packed bed can be described by the two-film theory as Eq. (3):

$$\frac{1}{K_G a_e} = \frac{1}{k_G a_e} + \frac{H}{I(k_L a_e)} \quad (3)$$

where H is the Henry's law constant expressed as the ratio of the partial pressure in the gas phase to the mass concentration in the liquid phase. The driving force between the saturated CO_2 concentration in the bulk gas and the CO_2 concentration on the surface of liquid film can be determined by mass balance over a thin shell of fluid with the RPB as shown in Eqs. (4) and (5):

$$\frac{1}{\rho_{CO_2}} \frac{dM_G}{dV} = K_G a_e (C_G^* - C_G') \quad (4)$$

$$dV = 2\pi r h \cdot dr \quad (5)$$

By substitution of Eq. (5) into Eq. (4), the overall gas-phase mass transfer coefficient can be obtained as Eq. (6):

$$K_G a_e = \frac{M_G}{\rho_G h\pi(r_o^2 - r_i^2)}(NTU_G) = \frac{Q_G}{h\pi(r_o^2 - r_i^2)} \ln\left(\frac{C_{G,i}}{C_{G,o}}\right) \quad (6)$$

Since the volumetric gas–liquid mass transfer coefficients in an RPB are an order of magnitude higher than those in a conventional packed bed, the volume of the RPB reactor is much smaller than that of a conventional reactor [9,10]. In addition, $K_G a$ increases with the gas flow rate, with the liquid flow rate, and mainly with the rotor speed [21].

Kelleher and Fair (1996) obtained an overall volumetric mass transfer coefficient in terms of the area of transfer unit (ATU) for the gas side from the literature [22]. HTU and ATU can be calculated from the experimental data using Eqs. (7) and (8), respectively [23]:

$$\mathrm{HTU} = \frac{r_o - r_i}{\mathrm{NTU}} = \frac{r_o - r_i}{\ln(C_{G,i}/C_{G,o})} \quad (7)$$

$$\mathrm{ATU} = \frac{\pi(r_o^2 - r_i^2)}{\mathrm{NTU}} = \frac{\pi(r_o^2 - r_i^2)}{\ln(C_{G,i}/C_{G,o})} \quad (8)$$

More information regarding development of the mass transfer model for high-gravity carbonation process can be found in the Appendix A.

3. Results and discussion

3.1. Effect of key operating factors on $K_G a$ and HTU

In this study, the effect of key operating factors such as rotating speed, L/S ratio, slurry flow rate, and gas flow rate on $K_G a$ and HTU values was evaluated. Fig. 1(a) and (b) present the effect of rotation speed, L/S ratio and slurry flow rate on $K_G a$ for high-gravity carbonation of BOFS–CRW, respectively. The rotation speed varied from 150 to 550 rpm, offering a centrifugal acceleration variation from 60 m/s^2 to 770 m/s^2. The $K_G a$ values were found to moderately increase with an increase of rotation speed (i.e., up to 300–500 rpm), indicating that the mass transfer resistance was reduced by an increasing rotation speed within this range. However, when the rotation speed increased beyond this range, a reduction in $K_G a$ was observed. This might be attributed to the fact that the extent of reduction in mass-transfer resistances at higher rotation speed was compensated for by a reduction of the retention time, which was unfavorable to carbonation reaction.

The $K_G a$ value was also found to be significantly affected by both the L/S ratio and the slurry flow rate. The results indicate that a superior $K_G a$ performance was achieved at a low L/S ratio, i.e., 10. In the case of a low L/S ratio, before carbonation occurs, the concentration of reactive species (e.g., Ca^{2+}) in the slurry solution should be higher than that under a high L/S ratio, leading to a stronger driving force of chemical potential for carbonation reaction. In addition, the $K_G a$ value was found to increase significantly with the increase of slurry flow rate. The $K_G a$ value was four times

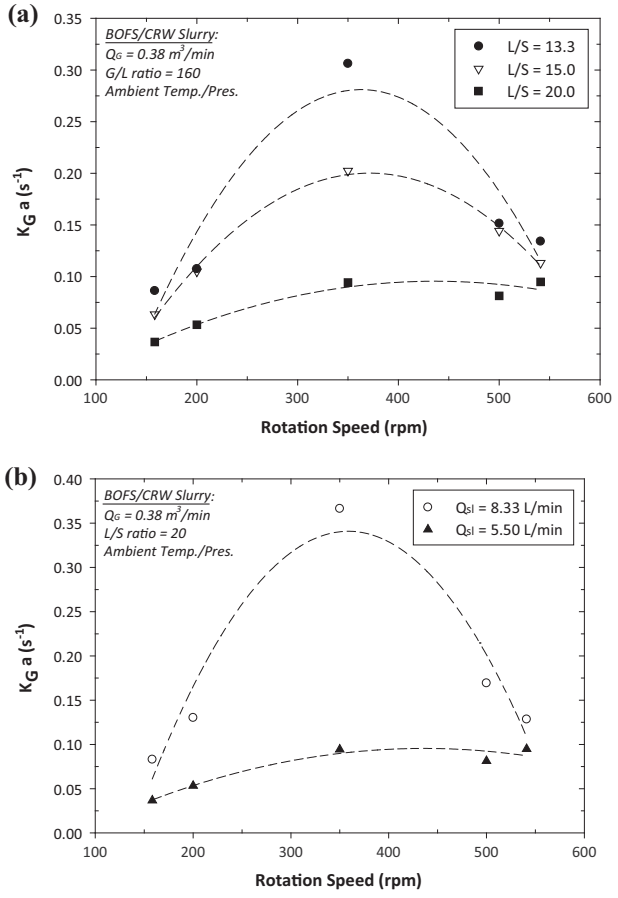

Fig. 1. Effect of (a) L/S ratio and (b) slurry flow rate on $K_G a$ for high-gravity carbonation of BOFS–CRW.

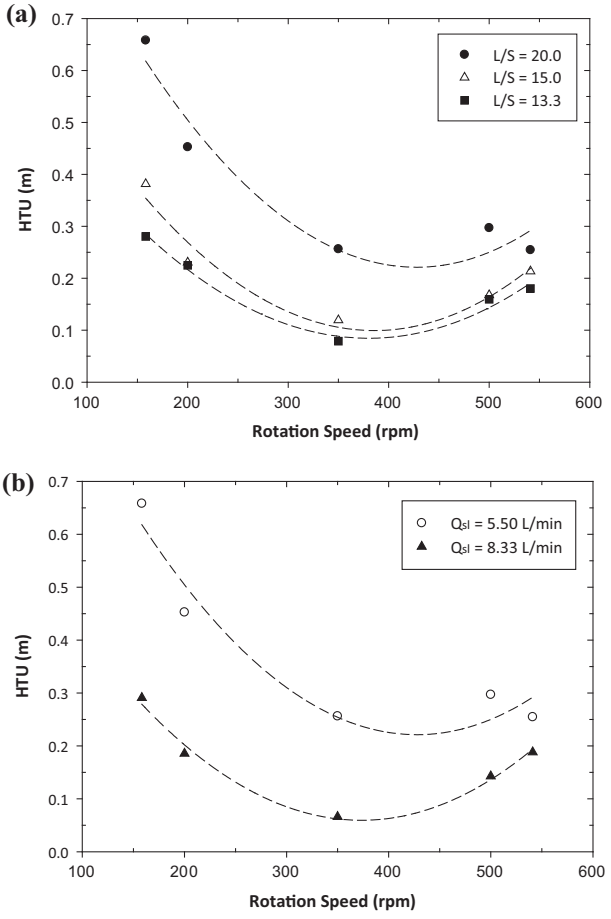

Fig. 2. Effect of rotation speed associated with (a) L/S ratio and (b) slurry flow rate on HTU value for high-gravity carbonation of BOFS–CRW.

higher (e.g., from 0.08 s^{-1} to 0.35 s^{-1}) if the slurry flow rate increased from 5.5 L/min to 8.3 L/min under a rotation speed of 350 rpm. This implies that the mass transfer limit of high-gravity carbonation is dependent on the liquid-phase side according to the two-film theory. It thus suggests that the turbulence resulted from rapid agitation or appropriate increases of rotation speed in an RPB may reduce the thickness of the liquid film, thereby lowering resistance of gaseous CO_2 to transfer into solution.

The HTU values of the high-gravity carbonation in an RPB were determined by Eq. (7) according to the HTU definition of a conventional packed bed. The HTU is a simple but representative design parameter for comparing the performance of a packed bed. The mass transfer performance of a packed bed can be dictated by the height of packing, e.g., $(r_o - r_i)$ in the case of an RPB, and the number of transfer units (NTU) that can be achieved in that height. A lower HTU value represents better mass transfer performance. Fig. 2 shows the effect of rotation speed, L/S ratio, and slurry flow rate on HTU value. The achievable stages are affected by the interfacial contact area, mass flux, and transport properties of the phases [9]. When the rotation speed of the bed is increased, the gas velocity and the packing specific surface area can both increase, thereby causing higher mass fluxes. However, a further increase in rotation speed will reduce the gas-slurry contacting time in the packed bed, thereby decreasing the CO_2 removal efficiency and HTU value. It was observed that a favorable rotation speed ranges between 300 rpm and 500 rpm to provide sufficient retention time for gas and liquid contacts. For a rotation speed of 350 rpm, the HTU value was found to be 7.8–28.0 cm with various L/S ratios between 13.3 and 20.0. Moreover, the HTU values were found to decrease with both a decrease in L/S ratio and an increase in the slurry flow rate.

Fig. 3 shows the effect of gas flow rate on K_Ga, which indicates that the gas flow rate has little effect on K_Ga. It was observed that the K_Ga decreased as the gas flow rate increased, which indicated that the carbonation of BOFS/CRW in an RPB should be a liquid-side mass transfer controlled reaction. Since an increase in gas–liquid contact area and a reduction in gas–liquid mass transfer resistance occur at higher gas flow rates, an overall decrease in K_Ga should result from a reduction of contact time. On the other hand, Fig. 4 shows the effect of gas and slurry flow rate on HTU value for the high-gravity carbonation process. The results indicate that an increase in gas flow rate results in a higher HTU value due to a lower retention time of gas in the packed zone. Regardless of the gas flow rate, the HTU proportionally decreases as the slurry flow rate increases, indicating a greater CO_2 removal efficiency. In contrast to the K_Ga value, the HTU value was not significantly affected by the G/L ratio. The G/L ratio is an important factor being commonly utilized for absorption process design. It was noted that

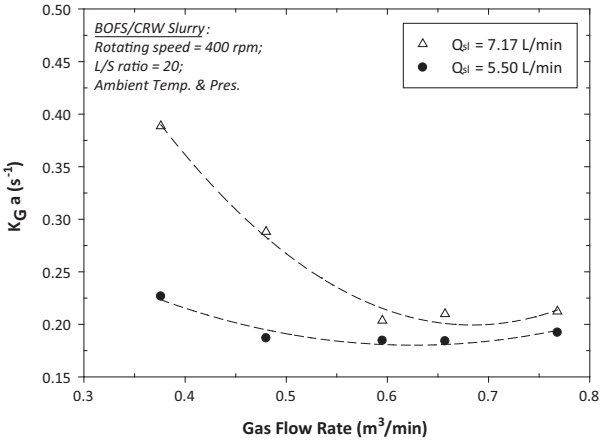

Fig. 3. Effect of gas and slurry flow rate on K_Ga for carbonation of BOFS-CRW.

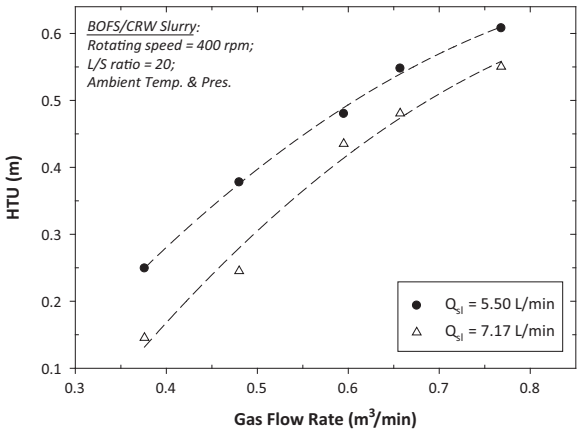

Fig. 4. Effect of gas and slurry flow rate on HTU value for carbonation of BOFS/CRW slurry.

Table 1
Mass transfer characteristics determined from two-film theory with their respective CO_2 capture efficiency under various operating conditions.

No	Operating conditions				η (%)[a]	Mass transfer characteristics			
	ω' (rpm)	Q_G (m^3/min)	Q_{sl} (L/min)	L/S (w/w)		K_Ga (1/s)	HTU (m)	NTU (–)	ATU (m^2)
1	158	0.38	5.50	20	27.3	0.037	0.658	0.319	0.858
2	200	0.38	5.50	20	37.1	0.053	0.453	0.464	0.590
3	350	0.38	5.50	20	55.9	0.094	0.256	0.819	0.334
4	500	0.38	5.50	20	50.7	0.081	0.297	0.707	0.387
5	541	0.38	5.50	20	56.2	0.095	0.255	0.825	0.332
6	158	0.38	8.33	20	51.4	0.083	0.291	0.722	0.379
7	200	0.38	8.33	20	67.8	0.130	0.186	1.132	0.242
8	350	0.38	8.33	20	95.9	0.366	0.066	3.183	0.086
9	500	0.38	8.33	20	77.0	0.169	0.143	1.471	0.186
10	541	0.38	8.33	20	67.2	0.128	0.188	1.116	0.245
11	350	0.38	6.67	20	71.3	0.144	0.168	1.247	0.220
12	350	0.38	9.33	20	97.3	0.416	0.058	3.613	0.076
13	158	0.38	5.50	15	42.3	0.063	0.382	0.550	0.498
14	200	0.38	5.50	15	59.8	0.105	0.230	0.912	0.300
15	350	0.38	5.50	15	82.8	0.202	0.119	1.759	0.156
16	400	0.38	5.50	15	98.3	0.468	0.052	4.068	0.067
17	450	0.38	5.50	15	86.4	0.229	0.105	1.993	0.137
18	500	0.38	5.50	15	71.4	0.144	0.168	1.253	0.219
19	541	0.38	5.50	15	62.6	0.113	0.214	0.984	0.278
20	158	0.38	6.67	13.3	65.0	0.121	0.200	1.049	0.261
21	200	0.38	6.67	13.3	65.1	0.121	0.200	1.052	0.260
22	350	0.38	6.67	13.3	95.8	0.365	0.066	3.172	0.086
23	500	0.38	6.67	13.3	96.9	0.401	0.060	3.488	0.079
24	541	0.38	6.67	13.3	88.0	0.244	0.099	2.122	0.129
25	200	0.38	9.33	13.3	99.5	0.603	0.040	5.239	0.052
26	350	0.38	9.33	13.3	99.6	0.645	0.037	5.608	0.049
27	500	0.38	9.33	13.3	99.4	0.596	0.041	5.181	0.053
28	400	0.38	5.50	20	56.9	0.097	0.249	0.842	0.325
29	400	0.48	5.50	20	42.6	0.082	0.378	0.556	0.493
30	400	0.60	5.50	20	35.4	0.080	0.480	0.437	0.626
31	400	0.66	5.50	20	31.8	0.077	0.548	0.383	0.714
32	400	0.77	5.50	20	29.2	0.081	0.608	0.345	0.793
33	400	0.38	7.17	20	76.4	0.166	0.145	1.444	0.190
34	400	0.48	7.17	20	57.5	0.126	0.245	0.856	0.320
35	400	0.60	7.17	20	38.3	0.088	0.435	0.483	0.567
36	400	0.66	7.17	20	35.4	0.088	0.481	0.437	0.627
37	400	0.77	7.17	20	31.7	0.090	0.550	0.382	0.718
38	350	0.38	5.50	15	63.2	0.115	0.210	0.999	0.274
39	350	0.48	5.50	15	49.7	0.101	0.306	0.687	0.398
40	350	0.60	5.50	15	44.4	0.107	0.358	0.586	0.467
41	350	0.66	5.50	15	34.0	0.084	0.505	0.416	0.658

[a] η (%) = CO_2 removal efficiency in flue gas, as determined by Eq. (2).

the high-gravity carbonation process could be operated at the higher G/L ratio, i.e., greater than 40, capturing a great amount of CO_2 in a relatively less slurry solution.

3.2. Model validation by experimental data

Table 1 summarized the CO_2 capture efficiency under key operating conditions and its associated mass transfer characteristics including K_Ga, HTU, NTU, and ATU values derived from two-film theory. The highest K_Ga value obtained from the developed model was 0.645 s^{-1} under the designed experimental conditions at 350 rpm, where the corresponding HTU value was 3.7 cm. Generally, the average HTU of traditional columns was 0.5–1.0 m, whereas the high-gravity process can potentially reduce this value to 2.8–8.0 cm [24]. In this study, the HTU values of carbonation using BOFS/CRW in an RPB were found to be 4–66 cm depending on the operating conditions, which were much lower than that using a fixed packed bed tower [25]. Consequently, the size of a CO_2 capture reactor could be significantly reduced if an RPB was applied, which would be beneficial to field CO_2 capture due to the limited available land in industry.

In this study, a correlation for K_Ga in an RPB was developed based on the assumption that K_Ga depends on the following parameters: gas diffusivity, gas superficial velocity, gas density, gas viscosity, liquid superficial velocity, liquid density, liquid viscosity, centrifugal acceleration, total specific surface area of packings, and effective diameter of packings. The following equations were obtained by the non-linear regression of experimental data for estimation of both the K_Ga and HTU values of the high-gravity carbonation process:

$$K_Ga_e = 0.01\left(\frac{a_tD_G}{d_p}\right)Re_G^{-1.16}Gr_G^{0.33}Re_L^{2.12} \quad (9)$$

$$\mathrm{HTU} = 0.0003\left(\frac{a_tD_G}{d_p}\right)Re_G^{2.16}Gr_G^{-0.33}Re_L^{-2.12} \quad (10)$$

where the ranges of the dimensionless groups in this correlation are as follows:

$$7.8 < Re_G < 15.9 \quad (11)$$

$$1.3 < Re_L < 2.2 \quad (12)$$

$$2.3 < Gr_G < 26.8 \quad (13)$$

Fig. 5 shows the comparison of the K_Ga value estimated by the developed model with the experimental data, which indicates that the K_Ga values predicted by the developed model were similar to the experimental value. The experimental K_Ga values lay within ±20% of the values estimated by Eq. (6). Both the K_Ga and HTU values varied with the centrifugal acceleration to the 0.33 power. As evidenced by Eq. (9), the dependence of liquid velocity on K_Ga value was much higher than that of gas velocity, indicating that the carbonation of BOFS/CRW in an RPB could exhibit a mass transfer resistance lay on the liquid side. In contrast, in the case of the HTU value, the effect of gas velocity was similar to that of liquid velocity. It was noted that the overall mass-transfer coefficient in an RPB, especially the liquid-side mass transfer coefficient (k_La), was greater than that in packed columns. Since the tangential gas velocity in the rotor is nearly the same as that in the packing zone, the gas-side mass transfer coefficient is believed to be in the same range as that of the conventional packed column [26]. It was reported in the literature that the k_La value for reaction using CRW with a BOFS particle size of less than 125 μm was 9.23×10^{-4} s^{-1} based on the shell mass balance model [16].

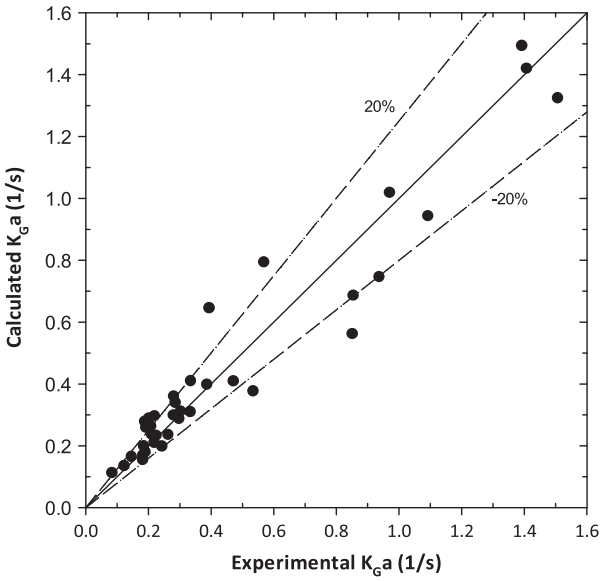

Fig. 5. Comparison of experimental and calculated K_Ga values of high-gravity carbonation process model developed in this study.

3.3. Establishment of response surface model

In order to optimize the mass transfer rate in the high-gravity carbonation process, a statistical K_Ga model was developed by the response surface methodology (RSM) according to the experimental data. A total of 40 experimental data was introduced in the RSM analysis. The important factors including rotation speed (coded as A), gas flow rate (B), slurry flow rate (C), and L/S ratio (D) would affect the carbonation conversion of BOFS in an RPB. The independent variables including rotating speed (158–541 rpm), gas flow rate (0.38–0.77 m^3/min), slurry flow rate (0.33–0.56 m^3/h), and L/S ratio (13.3–20.0 L/kg) were coded with low and high levels in D-optimal design.

The least-squares estimation was used to determine the model parameters in the approximating polynomial equation, representing the response surface of K_Ga value, with a cubic-order model. Table 2 presents the analysis of variance table (ANOVA) for the developed response surface model to predict the K_Ga values. In general, values of "Prob > F" less than 0.0500 indicate that model terms are significant, while values greater than 0.1000 indicate that the model terms are not significant. In this study, the model F-value of 27.0 implies that the model is significant; there is only a 0.01% chance that a "Model F-Value" this large could occur due to noise.

Table 2
Analysis of variance table (ANOVA) for response surface model of K_Ga values.

Source	Sum of squares	df	Mean square	F value	p-value Prob > F
Model	0.89	6	0.13	27.01	<0.0001
A: Rotation speed	0.028	1	0.028	6.06	0.019
B: Gas flow rate	0.053	1	0.053	11.29	0.020
C: Slurry flow rate	0.42	1	0.42	90.14	<0.0001
D: L/S ratio	0.22	1	0.22	47.12	<0.0001
AB	0.026	1	0.026	5.64	0.0235
A^2	0.082	1	0.082	17.44	0.0002
C^2	0.069	1	0.069	14.79	0.0005
Residual	0.15	33	0.0047		
Cor total	1.04	40			

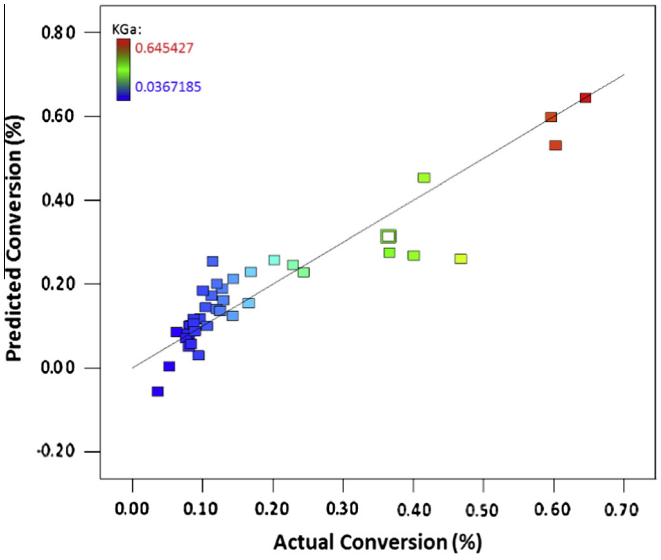

Fig. 6. Prediction versus actual values of response surface model for K_Ga values.

The analysis of the fitted response surface is generally equivalent to the analysis of the actual system if the fitted surface is a satisfactory estimation of the true response function. The developed model associated with rotation speed (A), gas flow rate (B), slurry flow rate (C), and L/S ratio (D) on overall gas-phase mass transfer coefficient (K_Ga) is presented in Eq. (14). The L/S ratio was found to exhibit a negative effect on the K_Ga value, while there was a dependent relationship between rotation speed and gas flow rate on the K_Ga value.

$$K_Ga(\text{coded}) = -0.13 + 1.32 * A - 0.71 * B - 0.16 * C - 0.14 * D + 2.04 * AB - 0.13 * A^2 + 0.11 * C^2 \quad (14)$$

Figs. 6 and 7 present the comparison of the predicted K_Ga value with the calculated K_Ga value, and the 2D contour plot of RSM model, respectively. A good fitting of the experimental data to response surface was observed with an R^2 value of 0.85 and a standard deviation of 0.068, which indicates that the K_Ga value could be well predicted by the RSM as expressed in Eq. (14). By changing the default values of slurry flow rate and L/S ratio, different 2D contour plots based on rotation speed and gas flow rate were obtained.

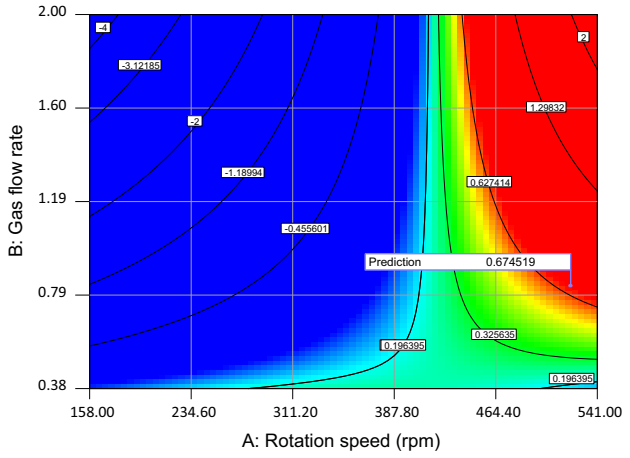

Fig. 7. 2D contour plot of K_Ga values (carbonation conditions: 521 rpm; Q_G = 0.82 m^3/min; Q_{sl} = 7.67 L/min, and L/S = 18.5).

Table 3
Candidates of optimal K_Ga solutions using RSM under different operating conditions and verified with theoretical model.

No	ω'[a] (rpm) (1)	Q_G[a] (m^3/min) (2)	Q_{sl}[a] (L/min) (3)	G/L ratio (–) (4)	L/S ratio (mL/g) (5)	K_Ga value (s^{-1})[b] Eq. (14) (6)	Eq. (9) (7)	RPD[c] (%)
1	462.1	0.33	9.33	35.4	10.12	0.670	0.672	0.3
2	462.7	0.34	9.33	36.4	10.61	0.656	0.650	0.9
3	505.1	0.82	6.50	126.2	12.35	0.708	0.715	1.0
4	487.3	0.44	9.17	48.0	11.21	0.687	0.680	1.0
5	534.4	0.72	6.33	113.7	12.77	0.672	0.632	6.1
6	360.2	0.42	9.00	46.7	10.06	0.651	0.699	7.1

[a] ω' = Rotation speed (rpm); Q_G = gas flow rate (m^3/min); Q_{sl} = slurry flow rate (L/min).
[b] Eq. (14) was obtained for RSM; Eq. (9) was determined based on theoretical model.
[c] RPD (relative percent difference) = |(6) – (7)|/{[(6) + (7)]/2}.

3.4. Optimization of gas-phase mass transfer rate

Several candidate optimal K_Ga values were obtained at different operating conditions by the developed RSM, as shown in Table 3. For instance, a candidate optimal solution of K_Ga value might be 0.67 s^{-1} operated under a gas flow rate of 0.33 m^3/min and a slurry flow rate of 9.33 L/min at a rotation speed of 462 rpm with an L/S ratio of 10.12. The candidate solutions were further verified by the theoretical model based on the two-film theory. The obtained RSM results were found to be in fairly good agreement with the results of the developed model by Eq. (9), with a relative percent difference (RPD) of less than 10%. It was thus concluded that the mass transfer characteristics in high-gravity carbonation can be optimized from both the theoretical approach (i.e., two-film theory) and the statistical approach (i.e., RSM).

Since the K_Ga value under different operating conditions can be successfully determined by Eq. (9), a correlation between CO_2 removal efficiency and K_Ga value can be established according to the definition of K_Ga in two-film theory and modified as Eq. (15):

$$\eta(\%) = \eta_{max}[1 - \exp(-t' \times K_Ga)] \quad (15)$$

The η_{max} value is the maximum CO_2 removal efficiency of the high-gravity carbonation process, which should have a theoretically maximum value of 100%. The exponential coefficient, i.e., t', can be regarded as the characteristic time of carbonation, which was approximately 7.10 ± 0.45 (s) with a determination coefficient (r^2) of 0.955, in the case of utilizing RPB. It was noted that the average residence time of liquid flow in an RPB was approximately 0.2–0.8 s [27]. Although the carbonation reaction rate was generally fast enough compared to the retention time of gas in an RPB, an appropriate level of G/L ratio should be maintained for the operation of high-gravity carbonation. At a constant slurry flow rate, an increase in gas flow rate, corresponding to a greater G/L ratio would reduce the retention time of gas in the packed bed zone.

In order to optimize the gas-phase mass transfer rate for the high-gravity carbonation process with a relatively lower energy consumption, the favorable operating modulus was systematically determined via graphical presentation, as shown in Fig. 8. The energy consumptions including RPB, blower, air compressor and pump were directly measured during operation and expressed in terms of kW h per ton CO_2 capture by the RPB. The result indicates that a centrifugal acceleration should be maintained at 475 m/s^2 for a relatively lower energy consumption (L1 → L2) and greater K_Ga value (L3 → L4). In addition, the favorable G/L ratio should range from 40–55 for high-gravity carbonation (determined by both L5 → L6 and R1 → R2 → R3). A further increase in G/L ratio up to 80 will lead to a low K_Ga value and high energy consumption

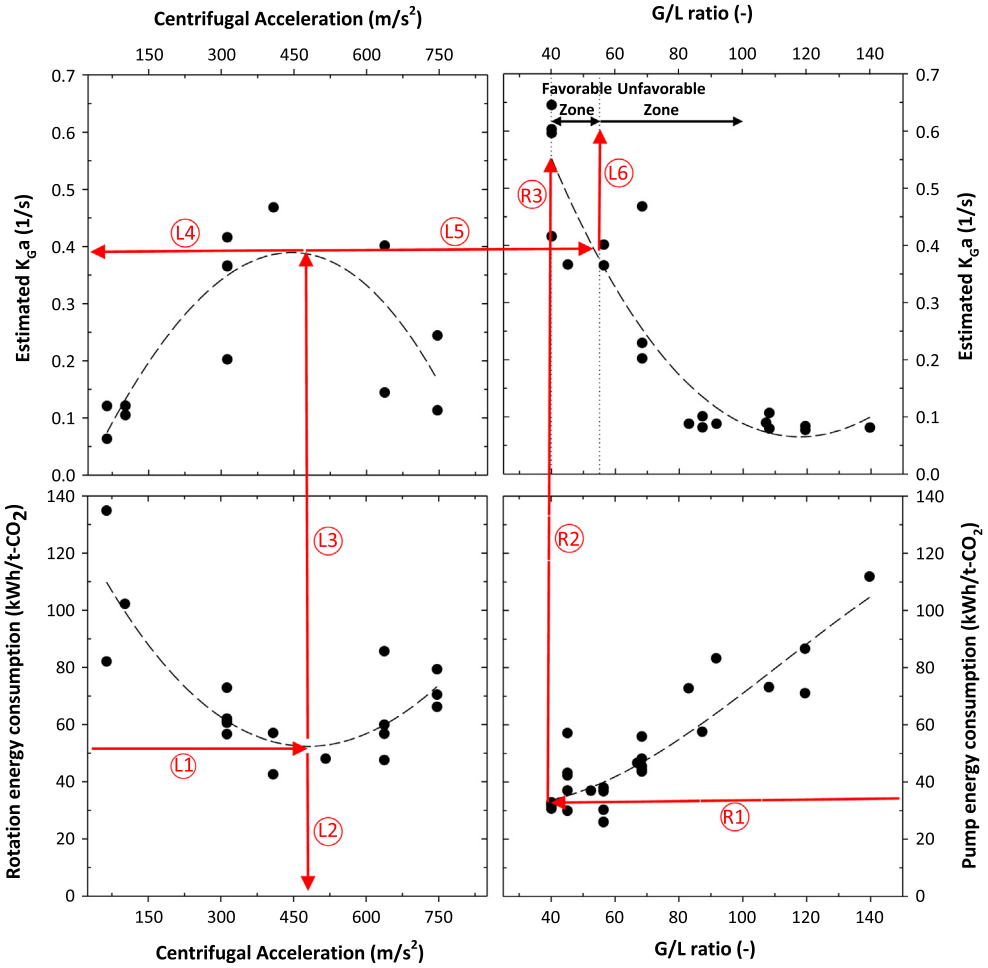

Fig. 8. Determination of optimal K_Ga value associated with favorable centrifugal acceleration (i.e., rotation speed) and G/L ratio via graphical presentation for high-gravity carbonation process (as indicated by red line). (For interpretation of the references to colour in this figure legend, the reader is referred to the web version of this article.)

for rotation and pumps, thereby exhibiting a poor CO_2 removal efficiency and capacity.

4. Conclusions

In this study, the optimum gas-phase mass transfer rate for the high-gravity carbonation process of steelmaking slags in an RPB was systematically determined from both theoretical considerations and statistical analyses of experimental data. The developed mass transfer model based on two-film theory was validated against experimental data and verified by the RSM. The highest experimental K_Ga value determined from the developed model was 0.645 s^{-1} at a rotation speed of 350 rpm, where the corresponding HTU value was 3.7 cm. Moreover, the mass transfer results showed that the HTU in a liquid-film limited system (i.e., carbonation) can be in the range of 4–66 cm at moderate centrifugal acceleration of 6–80 g. The results of theoretical dimensionless models also were compared to that obtained from RSM. One of the candidate optimal solutions of K_Ga value from RSM simulation was 0.67 s^{-1} operated under a gas flow rate of 0.33 m^3/min and a slurry flow rate of 9.33 L/min at a rotation speed of 462 rpm with an L/S ratio of 10.12. Furthermore, the energy consumptions of unit processes were included to obtain a compromise between CO_2 removal efficiency and energy consumption for process optimization. This suggests that a favorable G/L ratio for superior mass-transfer and energy consumption will be achieved at the range of 40–55 under a centrifugal acceleration of 475 m/s^2.

It was noted that an integrated approach to utilizing theoretical model and statistical analysis (i.e., RSM) for identification of the key operating parameters was investigated in this study. Furthermore, the future research should be focused on the changes of size and surface area of solid particles because part of the mineral might dissolve and reduce the particle size, and some of particles will collide each other, thereby breaking up into smaller particles and increasing the surface area during the carbonation.

Acknowledgements

High appreciation goes to Ministry of Science and Technology (MOST) of Taiwan (R.O.C.) for the financial support under Grant Number MOST 104-3113-E-007-001. In addition, Prof. H. Kim was supported by the R&D Program of MKE/KEIT (10037331, Development of Core Water Treatment Technologies based on Intelligent BT-NT-IT Fusion Platform).

Appendix A. Mass transfer model

Several studies have conducted different kinetic model to determine the rate-limiting step of mineral carbonation [2,28]. In fact, solid–liquid mass transfer is particularly important in mineral carbonation, and in many cases the rate limiting factor [18,29] because minerals in solid matrix dissolve partly, and passive layers are formed, gradually increasing resistance to mass transfer, and eventually leading to incomplete conversion. In general, the

solid–liquid mass-transfer coefficient is occasionally correlated as itself, where such correlations are specific to the system under consideration and are not generally applicable [29]. As the aforementioned, the mass transfer between liquid and solid phases in the high-gravity carbonation system was neglected in this study.

In addition, in spite of the significant differences between RPB and traditional packed column, penetration theory was still capable of describing the liquid-side mass transfer behavior fairly well in RPB [30]. These correlations are most often expressed in terms of dimensionless numbers in the form of a power series. For instance, penetration theory can be applied to RPB to yield as Eq. (A1):

$$k_L = 0.92\left(\frac{D_L}{d_p}\right) Sc_L^{1/2} Re_L^{1/3} Gr_L^{1/6} \tag{A1}$$

where the Grashof number which represents the ratio of gravitational to viscous forces can be determined by Eq. (A2), and the g value can be replaced by the centrifugal acceleration term as shown in Eq. (A3):

$$Gr_L = g d_p^3 \left(\frac{\rho_L}{\mu_L}\right)^2 \tag{A2}$$

$$g = a_m = \left(\frac{r_o^2 + r_i^2}{2}\right)^{1/2} \omega^2 \tag{A3}$$

Another commonly used prediction for liquid-side (k_L) and gas-side (k_G) mass transfer coefficient in a conventional packed column is that of Onda et al. (1968), as shown in Eqs. (A4) and (A5), respectively. Onda et al. suggested the constant of 5.23 of Eq. (A5) should be best correlated by changing the constant into 2.00 for smaller packings (i.e. diameter is less than 1.5 cm) since the $K_G a$ data for packings smaller than 1.5 cm tend to decrease in the literatures [31].

$$k_L = 0.0051\left(\frac{a_t}{a_w}\right)^{2/3} Re_L^{2/3} Sc_L^{-1/2} \left(\frac{\rho_L}{\mu_L g}\right)^{-1/3} (a_p d_p)^{0.4} \tag{A4}$$

and

$$k_G = 5.23(a_p D_G) Re_G^{0.7} Sc_G^{1/3} (a_p d_p)^{-2} \tag{A5}$$

It is usually difficult to obtain mass transfer coefficients separated from volumetric mass transfer coefficients $k_L a_e$ and $k_G a_e$ since the effective interfacial area between the liquid and vapor phase is usually not known [9]. Several correlations have been reported to estimate the wetted surface area (a_w), among which the Tung and Muh [30] found that the a_w/a_t predicted value by Perry and Chilton [32] is "reliable" under high-gravity RPB process as shown in Eq. (A6).

$$\frac{a_w}{a_t} = \frac{a_e}{a_t} = 1 - \exp\left[-1.45\left(\frac{\sigma_c}{\sigma_L}\right)^{0.75} Re_L^{0.1} We_L^{0.2} Fr_L^{-0.05}\right] \tag{A6}$$

The assumption of the above equality is that for packing materials with small static hold up (i.e., large packing size) the wetted area (a_w) may equal the interfacial area (a_e).

References

[1] Chang EE, Wang Y-C, Pan S-Y, Chen Y-H, Chiang P-C. CO_2 capture by using blended hydraulic slag cement via a slurry reactor. Aerosol Air Qual Res 2012;12:1433–43.

[2] Lekakh SN, Rawlins CH, Robertson DGC, Richards VL, Peaslee KD. Kinetics of aqueous leaching and carbonization of steelmaking slag. Metall Mater Trans B 2008;39:125–34.

[3] Pan S-Y, Chang EE, Chiang P-C. CO_2 capture by accelerated carbonation of alkaline wastes: a review on its principles and applications. Aerosol Air Qual Res 2012;12:770–91.

[4] Santos RM, François D, Mertens G, Elsen J, Van Gerven T. Ultrasound-intensified mineral carbonation. Appl Therm Eng 2013;57:154–63.

[5] Teir S, Eloneva S, Fogelholm C, Zevenhoven R. Fixation of carbon dioxide by producing hydromagnesite from serpentinite. Appl Energy 2009;86:214–8.

[6] Costa G, Baciocchi R, Polettini A, Pomi R, Hills CD, Carey PJ. Current status and perspectives of accelerated carbonation processes on municipal waste combustion residues. Environ Monit Assess 2007;135:55–75.

[7] Lin C, Chen B. Characteristics of cross-flow rotating packed beds. J Ind Eng Chem 2008;14:322–7.

[8] Wang M. Controlling factors and mechanism of preparing needlelike $CaCO_3$ under high-gravity environment. Powder Technol 2004;142:166–74.

[9] Kelleher T, Fair JR. Distillation studies in a high-gravity contactor. Ind Eng Chem Res 1996;35:4646–55.

[10] Tan C, Chen J. Absorption of carbon dioxide with piperazine and its mixtures in a rotating packed bed. Sep Purif Technol 2006;49:174–80.

[11] Chang EE, Pan SY, Chen YH, Tan CS, Chiang PC. Accelerated carbonation of steelmaking slags in a high-gravity rotating packed bed. J Hazard Mater 2012;227–228:97–106.

[12] Pan SY, Chiang PC, Chen YH, Chen CD, Lin HY, Chang EE. Systematic approach to determination of maximum achievable capture capacity via leaching and carbonation processes for alkaline steelmaking wastes in a rotating packed bed. Environ Sci Technol 2013;47:13677–85.

[13] Pan SY, Chiang PC, Chen YH, Tan CS, Chang EE. Ex Situ CO_2 capture by carbonation of steelmaking slag coupled with metalworking wastewater in a rotating packed bed. Environ Sci Technol 2013;47:3308–15.

[14] Xiang Y, Wen LX, Chu GW, Shao L, Xiao GT, Chen JF. Modeling of the precipitation process in a rotating packed bed and its experimental validation. Chin J Chem Eng 2010;18:249–57.

[15] Chen YH, Huang YH, Lin RH, Shang NC. A continuous-flow biodiesel production process using a rotating packed bed. Bioresour Technol 2010;101:668–73.

[16] Chang EE, Chen T-L, Pan S-Y, Chen Y-H, Chiang P-C. Kinetic modeling on CO_2 capture using basic oxygen furnace slag coupled with cold-rolling wastewater in a rotating packed bed. J Hazard Mater 2013;260:937–46.

[17] Pan S-Y, Chiang P-C, Chen Y-H, Tan C-S, Chang EE. Kinetics of carbonation reaction of basic oxygen furnace slags in a rotating packed bed using the surface coverage model: maximization of carbonation conversion. Appl Energy 2014;113:267–76.

[18] Munjal S, Dudukovic MP, Ramachandran P. Mass-transfer in rotating packed beds – I. Development of gas–liquid and liquid–solid mass transfer correlations. Chem Eng Sci 1989;44:2245–56.

[19] Zhao B, Su Y, Tao W. Mass transfer performance of CO_2 capture in rotating packed bed: dimensionless modeling and intelligent prediction. Appl Energy 2014;136:132–42.

[20] Chang EE, Chiu A-C, Pan S-Y, Chen Y-H, Tan C-S, Chiang P-C. Carbonation of basic oxygen furnace slag with metalworking wastewater in a slurry reactor. Int J Greenhouse Gas Control 2013;12:382–9.

[21] Liu H, Kuo C. Quantitative multiphase determination using the Rietveld method with high accuracy. Mater Lett 1996;26:171–5.

[22] Sandilya P, Rao DP, Sharma A. Gas-phase mass transfer in a centrifugal contactor. Ind Eng Chem Res 2001;40:384–92.

[23] Cheng H-H, Shen J-F, Tan C-S. CO_2 capture from hot stove gas in steel making process. Int J Greenhouse Gas Control 2010;4:525–31.

[24] Martin CL. Preliminary distillation mass transfer and pressure drop results using a pilot-plant scale high gravity contacting unit. AIChE Spring National Meeting. New Orleans, LA; 1992.

[25] Yu C-H, Huang C-H, Tan C-S. A Review of CO_2 capture by absorption and adsorption. Aerosol Air Qual Res 2012;12:745–69.

[26] Chandra A, Goswami PS, Rao DP. Characteristics of flow in a rotating packed bed (HIGEE) with split packing. Ind Eng Chem Res 2005;44:4051–60.

[27] Guo K, Guo F, Feng Y, Chen J, Zheng C, Gardner NC. Synchronous visual and RTD study on liquid flow in rotating packed-bed contactor. Chem Eng Sci 2000;55:1699–706.

[28] Chang EE, Chen CH, Chen YH, Pan SY, Chiang PC. Performance evaluation for carbonation of steel-making slags in a slurry reactor. J Hazard Mater 2011;186:558–64.

[29] Arters DC, Fan L-S. Experimental methods and correlation of solid liquid mass transfer in fluidized beds. Chem Eng Sci 1986;41:107–15.

[30] Tung HH, Mah RSH. Modeling liquid mass transfer in HIGEE separation process. Chem Eng Commun 1985;39:147–53.

[31] Onda K, Takeuchi H, Okumoto Y. Mass transfer coefficients between gas and liquid phases in packed columns. J Chem Eng Jpn 1968;1:56–62.

[32] Perry RH, Chilton CH. Chemical engineers' handbook. New York: McGraw-Hill; 1973.